



Original Article

Chemomechanically Tuned Li–In/Sn Intermetallic Anodes for Sulfide SSBs: Composition–Transport Coupling and Pressure–Stabilized Interfaces

Samarth Patel
Independent Researcher, USA.

Received On: 06/12/2025

Revised On: 07/01/2026

Accepted On: 15/01/2026

Published On: 21/01/2026

Abstract - Intermetallic Li–In and Li–Sn anodes with high lithium content are engineered to sustain intimate, crack-resistant contact with Li₆PS₅Cl under optimized stack pressure, enabling dendrite-free cycling at 1 mA cm⁻² over thousand-hour timescales. The paper links composition-dependent lithium migration barriers to measured overpotentials through combined atomistic modeling and electrochemical testing, revealing how phase selection (e.g., Li₁₃In₃, Li₁₇Sn₄) governs transport and interfacial kinetics. Controlled synthesis and fabrication routes yield robust chemomechanical coupling at the alloy–sulfide interface, suppressing interfacial degradation pathways that typically initiate filament growth. These materials-centric insights provide a design map connecting alloy stoichiometry, interphase stability, and processing pressure to durable solid-state battery operation, emphasizing scalable materials processing and interface engineering over cell-level optimization.

Keywords - Solid-State Batteries, Intermetallic Anodes, Li–In Alloys, Li–Sn Alloys, Interfacial Chemomechanics, Stack Pressure, Migration Barriers, and Sulfide Electrolytes.

1. Introduction

Solid-state batteries (SSBs) offer a transformative leap in energy density and safety by replacing flammable liquid electrolytes with solid counterparts. However, the integration of high-capacity anodes, particularly lithium metal, is hindered by severe interfacial chemomechanical instabilities that lead to dendritic short circuits and cell failure [1], [2]. These challenges are exacerbated by poor interfacial contact, large volume changes, and chemical incompatibility with solid electrolytes (SEs) [3], [4]. To circumvent these issues, lithium alloys have emerged as promising anode alternatives, offering improved dimensional stability and reduced reactivity with SEs [5], [6]. Among them, Li–In and Li–Sn systems have garnered attention due to their favorable electrochemical properties and compatibility with sulfide-based electrolytes like Li₆PS₅Cl [7], [8]. Nevertheless, prior studies have predominantly focused on low-Li-content alloys (e.g., Li_{0.5}In), which suffer from limited capacity and high cost due to the indium content [9]. High-Li-content phases such as Li₁₃In₃ and Li₁₇Sn₄ offer greater practical appeal but remain underexplored in terms of

their fundamental electro-chemo-mechanical behavior. This work systematically investigates a range of Li–In and Li–Sn alloys with varying Li stoichiometries, combining controlled synthesis, electro-chemical characterization, and computational modeling to unravel the interplay between composition, Li-transport kinetics, and interfacial stability. We demonstrate that high-Li-content alloys, when processed under optimal stack pressure, exhibit exceptional long-term cycling stability and minimal interfacial degradation, providing a viable pathway toward high-performance SSB anodes.

2. Related Work

Recent advancements in machine learning (ML) and deep learning (DL) offer powerful computational tools that can complement and accelerate research in materials science and solid-state battery design. In the domain of neural network optimization, demonstrates methods to enhance convergence in fully connected networks through vectorized backpropagation, normalization, and activation tuning techniques that could improve the efficiency of surrogate models for predicting battery material properties such as Li-migration barriers or phase stability. Concurrently, the work of [10]–[12] addresses the integration of multimodal data, interpretability, and reproducible pipelines. Specifically, [12] introduces a scalable fusion-attention framework for joint reasoning across time-series, image, and text data, which is highly relevant for correlating electrochemical, structural, and imaging data in battery research. Similarly, [11] proposes energy-guided counterfactual generation for faithful model interpretation, a method that could help elucidate the causal relationships between alloy composition, interfacial stability, and electrochemical performance.

Further ML contributions emphasize robustness, automation, and multi-objective optimization in real-world systems. [?] focuses on synthetic content detection using adaptive networks, highlighting approaches to feature extraction and authenticity verification that parallel the need for reliable detection of interfacial degradation in battery materials. [?] presents an adaptive security orchestration framework for intelligent policy enforcement via feedback-driven automation—a con-

cept that could inspire dynamic control systems for optimizing stack pressure or cycling conditions during battery operation. Finally, [13] incorporates fairness constraints directly into hyperparameter tuning, demonstrating how auxiliary objectives can be balanced with predictive accuracy. In battery design, such multi-objective optimization could jointly address trade-offs between capacity, kinetics, cost, and interfacial stability, ensuring that developed anodes meet both performance and practical manufacturing constraints.

3. Experimental Methods

3.1. Materials Synthesis

$\text{Li}_6\text{PS}_5\text{Cl}$ was synthesized via ball-milling and subsequent heat treatment, following established protocols [14]. The Li-In and Li-Sn alloys were prepared by solid-state reaction of stoichiometric amounts of Li (Sigma-Aldrich, 99.9%) and In/Sn (Alfa Aesar, 99.99%) sealed in evacuated quartz ampoules. The mixtures were heated stepwise to 400°C and held for 48 h to ensure complete intermetallic formation. The resulting ingots were then subjected to high-energy ball-milling (300 rpm, 180 min) to obtain fine powders. Phase purity was verified by X-ray diffraction (XRD, Bruker D8 Advance) using a Kapton-protected sample holder to prevent air exposure. The milled powders were pressed into foil-like electrodes under 150 MPa for electrochemical testing.

3.2. Electrochemical Characterization

Solid-state cells were assembled in a symmetric configuration (Alloy| $\text{Li}_6\text{PS}_5\text{Cl}$ |Alloy) using a homemade nylon die. Electrolyte pellets (12 mm diameter) were prepared by pressing 150 mg of $\text{Li}_6\text{PS}_5\text{Cl}$ powder at 510 MPa. Alloy electrodes were spread evenly on both sides of the pellet, and the stack was compressed under a controlled assembly pressure (150 MPa for alloys, 5 MPa for Li metal). Stack pressures during testing were maintained using a torque-controlled vice. Electrochemical impedance spectroscopy (EIS) was performed with a Biologic SP200 analyzer (7 MHz–100 mHz, 10 mV perturbation). Galvanostatic stripping/plating tests were conducted at current densities ranging from 50 to 1000 $\mu\text{A cm}^{-2}$ with a capacity limit of 1 mAh cm^{-2} . Long-term cycling was carried out at 1 mA cm^{-2} for up to 1000 h.

3.3. Computational Methodology

Density functional theory (DFT) calculations were performed using the Vienna Ab initio Simulation Package (VASP) with the projector-augmented wave method and the PBEsol functional. Formation energies were computed relative to the elemental phases, and convex hulls were constructed to identify stable intermetallics. Li-migration barriers were determined using the nudged elastic band (NEB) method with a dilute-vacancy model. Structural models were obtained from the Inorganic Crystal Structure Database (ICSD) and the Materials Project [15].

4. Results and Discussion

4.1. Alloy Synthesis and Structural Characterization

It illustrates the binary phase diagrams of Li-In and

Li-Sn systems, highlighting the selected low- ($\text{Li}_{0.5}\text{In}$, Li_2Sn_5), medium- (LiIn , LiSn), and high-Li-content ($\text{Li}_{13}\text{In}_3$, $\text{Li}_{17}\text{Sn}_4$) phases. XRD patterns confirm the phase-pure synthesis of all alloys after ball-milling. The high-Li phases exhibit peak broadening due to lattice strain induced by mechanical milling, whereas low-Li phases retain sharper reflections. SEM images reveal the transformation from coarse as-synthesized chunks to fine, uniform powders after milling, which is critical for achieving smooth electrode surfaces and intimate interfacial contact.

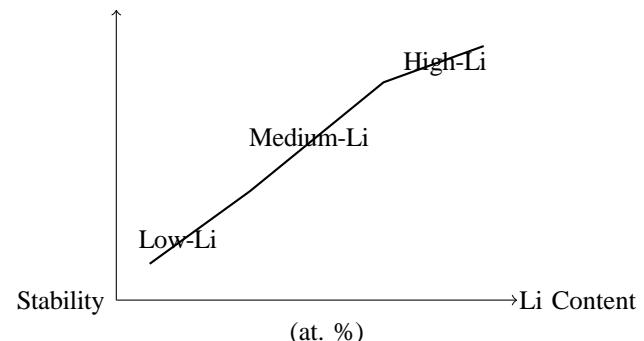


Fig 1: Li-In Phase Diagram

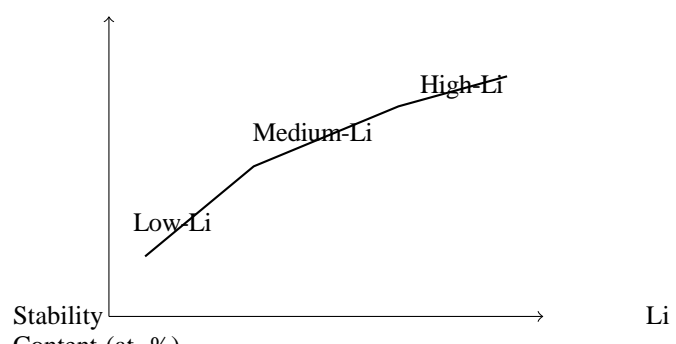


Fig 2: Li-Sn Phase Diagram

Fig. 1: Binary phase diagrams for (a) Li-In and (b) Li-Sn systems, indicating the regions of low-, medium-, and high-Li-content intermetallics.

4.2. Interfacial Contact and Stack-Pressure Effects

The evolution of the anode/SE interface during Li stripping was investigated under two stack pressures: 0 MPa and 45 MPa. It presents the potential profiles and impedance changes for Li metal and selected alloys. At 0 MPa, Li metal exhibits rapid interfacial void formation, leading to a dramatic increase in interfacial resistance (from 92 Ω to 54 k Ω) after stripping. In contrast, the alloys show a much smaller impedance rise due to the retained host-matrix contact. Under 45 MPa, the interfacial resistance remains negligible (~38 Ω) for all alloys, indicating nearly perfect contact. The stripped capacity improves significantly under pressure, highlighting the critical role of stack pressure in maintaining interfacial integrity and enabling higher Li utilization.

4.3. Computational Insights into Li Migration Barriers

DFT-computed formation energies and convex hulls for Li-In and Li-Sn systems. The stable phases identified ($\text{Li}_{13}\text{In}_3$, $\text{Li}_{17}\text{Sn}_4$, etc.) align well with experimental observations. Li-migration barriers, calculated via NEB, reveal strong composition dependence. In Li-In alloys, the barrier increases with Li content (34 meV for LiIn , 172 meV for $\text{Li}_{13}\text{In}_3$), whereas in Li-Sn alloys, the barrier decreases with Li content (434 meV for Li_2Sn_5 , 263 meV for $\text{Li}_{17}\text{Sn}_4$). These trends correlate directly with the experimentally observed overpotentials during symmetric cycling. The lower coordination number of Li in high-Li phases (e.g., 6–8 in $\text{Li}_{17}\text{Sn}_4$ vs. 8–10 in Li_2Sn_5) facilitates faster Li transport, contrary to typical design rules for oxide/sulfide hosts.

4.5. Symmetric Cycling Performance

Galvanostatic cycling of symmetric cells reveals distinct behaviors for different alloys. $\text{Li}_{0.5}\text{In}$ exhibits minimal polarization due to its biphasic (de)lithiation mechanism, while LiIn shows a sloped profile reflecting composition-dependent potential drift. High-Li phases $\text{Li}_{13}\text{In}_3$ and $\text{Li}_{17}\text{Sn}_4$ display stable plateau-like profiles with moderate overpotentials (180 mV and 440 mV, respectively, at 1 mA cm^{-2}). The Sn-based alloys generally suffer from higher polarization due to their larger migration barriers, consistent with computational predictions. Impedance measurements before and after cycling confirm excellent interfacial stability, with only minor increases in stack resistance.

4.6. Long-Term Cycling Stability

Long-term cycling tests (1000 h at 1 mA cm^{-2} , 1 mAh cm^{-2}) demonstrate exceptional stability for high-Li-content alloys. $\text{Li}_{13}\text{In}_3$ maintains a steady overpotential of ~180 mV with negligible impedance growth. $\text{Li}_{17}\text{Sn}_4$ shows a gradual overpotential increase from 440 mV to 650 mV over the first 300 h, after which it stabilizes, likely due to passivation layer formation. The impedance rise is modest (from 38 Ω to 65 Ω), confirming robust interfacial chemomechanics. These results underscore the viability of high-Li alloys for durable SSB operation under practical current densities.

5. Conclusions

This study establishes a comprehensive framework for designing high-performance Li-In and Li-Sn alloy anodes for sulfide-based SSBs. Through controlled synthesis, we achieved phase-pure intermetallics with tailored Li stoichiometries. The application of optimal stack pressure (45 MPa) ensures intimate interfacial contact, mitigating void formation and preserving electrochemical stability. Computational modeling reveals composition-dependent Li-migration barriers that directly govern cycling overpotentials: in Li-In alloys, barriers increase with Li content, while in Li-Sn alloys, they decrease. High-Li phases ($\text{Li}_{13}\text{In}_3$, $\text{Li}_{17}\text{Sn}_4$) offer an attractive balance of capacity, cost, and kinetics, enabling stable, dendrite-free cycling at 1 mA cm^{-2} for over 1000 h. Future work should focus on nano-structuring and composite designs to further enhance

Li-utilization and rate capability. These findings provide a materials-centric roadmap for advancing alloy-based anodes, addressing key chemomechanical challenges at the anode–SE interface.

References

- [1] M. D. Tikekar, S. Choudhury, Z. Tu, And L. A. Archer, “Design Principles For Electrolytes And Interfaces For Stable Lithium-Metal Batteries,” *Nature Energy*, Vol. 1, P. 16114, 2016.
- [2] K. B. Hatzell, X. C. Chen, C. L. Cobb, N. P. Dasgupta, M. B. Dixit, L. E. Marbella, M. T. McDowell, P. P. Mukherjee, A. Verma, V. Viswanathan,
- [3] S. Westover, And W. G. Zeier, “Challenges In Lithium Metal Anodes For Solid-State Batteries,” *Acs Energy Letters*, Vol. 5, Pp. 922–934, 2020.
- [4] T. Krauskopf, F. H. Richter, W. G. Zeier, And J. Janek, “Physicochemical concepts of the lithium metal anode in solid-state batteries,” *Chemical Reviews*, vol. 120, pp. 7745–7794, 2020.
- [5] J. A. Lewis, F. J. Q. Cortes, Y. Liu, J. C. Miers, A. Verma, B. S. Vishnugop, J. Tippens, D. Prakash, T. S. Marchese, S. Y. Han, C. Lee,
- [6] P. P. Shetty, H. Lee, P. Shevchenko, F. De Carlo, C. Saldana, P. P. Mukherjee, and M. T. McDowell, “Linking void and interphase evolution to electrochemistry in solid-state batteries using operando x-ray tomography,” *Nature Materials*, vol. 20, pp. 503–510, 2021.
- [7] W. D. Richards, L. J. Miara, Y. Wang, J. C. Kim, and G. Ceder, “Interface stability in solid-state batteries,” *Chemistry of Materials*, vol. 28, pp. 266–273, 2016.
- [8] T. K. Schwietert, V. Arszelewska, C. Wang, C. Yu, A. Vasileiadis,
- [9] N. J. J. de Klerk, J. Hageman, T. Hupfer, I. Kerkamm, Y. Xu, E. van der Maas, E. M. Kelder, S. Ganapathy, and M. Wagemaker, “Clarifying the relationship between redox activity and electrochemical stability in solid electrolytes,” *Nature Materials*, vol. 19, pp. 428–435, 2020.
- [10] A. L. Santhosha, L. Medenbach, J. R. Buchheim, and P. Adelhelm, “The indium–lithium electrode in solid-state lithium-ion batteries: Phase formation, redox potentials, and interface stability,” *Batteries & Supercaps*, vol. 2, pp. 524–529, 2019.
- [11] L. Zhou, K. Park, X. Sun, F. Lalere, T. Adermann, P. Hartmann, and
- [12] L. F. Nazar, “Solvent-engineered design of argyrodite $\text{Li}_6\text{PS}_5\text{X}$ (x = cl, br, i) solid electrolytes with high ionic conductivity,” *ACS Energy Letters*, vol. 4, pp. 265–270, 2018.
- [13] T. T. Werner, G. M. Mudd, and S. M. Jowitt, “Indium: Key issues in assessing mineral resources and long-term supply from recycling,” *Applied Earth Science*, vol. 124, pp. 213–226, 2015.
- [14] A. Agarwal, “A unified machine learning framework for enterprise portfolio forecasting, risk detection, and automated reporting,” *Preprints*, 2025.

- [15] "Energy-guided counterfactual generation for faithful model interpretation," *Preprints*, 2025.
- [16] "Neurofusionx: A scalable multi-modal deep learning framework with attention based fusion across healthcare, finance, and cybersecurity," *International Journal of Applied Mathematics*, vol. 38, no. 4s, 2025.
- [17] M. A. Nadeem, "Optimizing fairness in machine learning: A hyperparameter tuning approach," in *2025 IEEE Conference on Innovations in Software Engineering (COINS)*, 2025.
- [18] C. Hansel and D. Kundu, "The stack pressure dilemma in sulfide electrolyte based li metal solid-state batteries: A case study with $Li_6P_{5}Cl$ solid electrolyte," *Advanced Materials Interfaces*, vol. 8, p. 2100206, 2021.
- [19] A. Jain, S. P. Ong, G. Hautier, W. Chen, W. D. Richards, S. Dacek,
- [20] S. Cholia, D. Gunter, D. Skinner, G. Ceder, and K. A. Persson, "Commentary: The materials project: A materials genome approach to accelerating materials innovation," *APL Materials*, vol. 1, p. 011002, 2013.